IEEE Access
Multidisciplinary | Rapid Review | Open Access Journal

Received May 30, 2020, accepted June 11, 2020, date of publication June 16, 2020, date of current version June 26, 2020.

Digital Object Identifier 10.1109/ACCESS.2020.3002802

Safety Monitoring by a Graph-Regularized Semi-Supervised Nonnegative Matrix Factorization With Applications to a Vision-Based Marking Process

SONG FAN[1,2], QILONG JIA[1], AND WAN SHENG CHENG[2]
[1]College of Information Science and Engineering, Northeastern University, Shenyang 110819, China
[2]School of Electronic and Information Engineering, University of Science and Technology Liaoning, Anshan 114051, China

Corresponding author: Wan Sheng Cheng (cws_hit@126.com)

This work was supported by the National Natural Science Foundation of China under Grant 61733003.

ABSTRACT This paper proposes a brand-new method to perform safety monitoring using images for steel coil marking industrial processes. The new safety monitoring method is developed with the aid of a new graph-regularized semi-supervised nonnegative matrix factorization (GSNMF) algorithm. Compared with the existing nonnegative matrix factorization (NMF)-like algorithms, GSNMF is developed in an all-new manner so that it not only can take advantage of images with known labels and images with unknown labels to train a model for monitoring purpose, but also can take advantage of graph theory to improve the monitoring performance. Because any two different samples are connected by an edge in a graph, thus graph theory is beneficial for GSNMF to measure the similarity between any two different samples and to assign the same labels for the samples with close connections between them. As a result, GSNMF is more capable of analyzing the samples with a complicated distribution than the existing NMF-like algorithms, theoretically. Finally, an experiment on a steel coil marking process is adopted to evaluate the superiorities of our proposed method over the existing methods.

INDEX TERMS Fault detection, nonnegative matrix factorization, semi-supervised learning, marking process.

I. INTRODUCTION

The Safety of the workers is the hottest topic discussed in the field of engineering technology. Although people already made a lot of effort to protect workers from injury by robots over the past decades, the workers in the steel factory with robots still suffer from a high safety risk. The automatic marking system is an advanced production and processing equipment with industrial robots as the core equipment. Robots can replace workers to work continuously in the environment of high temperature, high noise, and toxic and harmful gases. As a result, robots have been widely used in the fields of aerospace, automobile manufacturing and iron and steel metallurgy. For the safety concern, workers should keep a safe distance from the robots [1], [2]. Compared with the traditional safety monitoring methods, the vision-based safety monitoring methods can provide a more intuitive monitoring result, which takes advantage of digital imaging techniques to monitor the work zone of robots and alerts the workers who suffer from safety risks. Traditionally, the safety officer observed many monitoring screens to find the potential safety risk in a factor. However, when dangers occurs, the safety officer may fail to find it in time due to negligence. Moreover, even he found a danger, it is still a hard task to generate alerts. Therefore, the vision-based safety monitoring methods are effective ways to solve this problem, where vision-based safety monitoring methods do not rely on the use of system models, and they are feasible if some samples are available in advance [3]–[7]. As a result, vision-based safety monitoring methods are much easier to implement compared with the traditional safety monitoring and fault detection techniques [8]–[12].

Recently, fault detection and isolation techniques have earned great progress in industrial applications. For example,

The associate editor coordinating the review of this manuscript and approving it for publication was Fanbiao Li.

Wu *et al.* proposed a fault detection filtering for complex systems over communication networks subject to nonhomogeneous Markovian parameters, where event-triggered scheme is used by the authors to decide whether the networks should be updated at the trigger instants [13]. Nonnegative matrix factorization (NMF) proposed by Lee and Seung has been used in the field of data science [14]. NMF is a matrix factorization algorithm, which has a lot of valuable features, such as data clustering. NMF has been applied in the fields of document clustering, image processing, and voice analysis [15]. People were attempting to explore the industrial applications of NMF over the past decades, such as fault detection and safety monitoring. A lot of successful industrial applications of NMF can be found. For example, Li *et al.* proposed a modified NMF algorithm, then this NMF algorithm is used to develop a fault detection approach [16]. In addition, Li *et al.* also applied NMF to the fault detection for the non-Gaussian process and the well-known benchmark Tennessee Eastman process [17], [18]. Recently, Jia *et al.* further exploited the clustering feature of NMF-like models to develop approaches for simultaneous fault detection and isolation [19]. Zhang *et al.* propose an adaptive graph regularization discriminant nonnegative matrix factorization for image clustering [20].

The main contributions of our manuscript are that the proposed GSNMF algorithm can fully make use of the labelled samples to implement semi-supervised learning in the framework of NMF, and the geometry of sample data is maintained in the GSNMF model at the same time because GSNMF incorporates a graph regularizer. Cai *et al.* [21] already proved that a graph regularizer can maintain the geometry structure of sample data. In addition, the nonlinear structure of sample data can be described as well with GSNMF, and the low dimensional representation of samples have a better separability. These merits of GSNMF make it become a powerful algorithm for data representation. As a result, the GSNMF-based safety monitoring approach can significantly improve safety monitoring performance theoretically.

The remainder of this article is organized as follows. The next section consists of the introduction to the GSNMF algorithm and the detailed proof of its convergence. In the section III, we will introduce the proposed GSNMF's application to developing a safety monitoring approach by identifying the membership of the current sample. A case study on a steel coil marking process will be made in the section IV to evaluate the monitoring performance of the proposed approach. In the last section, conclusions are summarized.

II. INTRODUCTION TO THE GSNMF ALGORITHM

Let us begin with a brief introduction to the semi-nonnegative matrix factorization (SNMF) algorithm. SNMF can be represented by the following matrix factorization model

$$\mathbf{X} = \mathbf{U}\mathbf{V} + \mathbf{E} \tag{1}$$

where matrix $\mathbf{X} \in \mathbb{R}^{m\times n}$, $\mathbf{U} \in \mathbb{R}^{m\times k}$, $\mathbf{V} \in \mathbb{R}_+^{k\times n}$, $\mathbf{E} \in \mathbb{R}^{m\times n}$ [23]. SNMF has a close relation with k-means clustering algorithm, which means SNMF can partition a set of samples into k clusters. It needs to emphasize that k denotes the cluster quantity of training samples, and can be set manually for purpose. SNMF and k-means have the same objective as follows to be minimized.

$$J(\mathbf{U}, \mathbf{V}) = \frac{1}{2}\|\mathbf{X} - \mathbf{U}\mathbf{V}\|_F^2 \tag{2}$$

After matrices $\mathbf{U} \in \mathbb{R}^{m\times k}$ and $\mathbf{V} \in \mathbb{R}_+^{k\times n}$ are determined by minimizing above objective function $J(\mathbf{U}, \mathbf{V})$, the memberships of the original samples in matrix $\mathbf{X}$ can be identified by the membership indicator matrix $\mathbf{V}$ [21], [22]. Every single detail about the clustering principles of SNMF can be found in the literature [23].

Next, we will propose a modified SNMF algorithm, which is referred to as graph-regularized semi-supervised nonnegative matrix factorization (GSNMF). In fact, Cai's work [21] inspires us in part to develop GSNMF algorithm with applications to safety monitoring. GSNMF is developed deliberately with the aid of graph theory for analyzing samples with a complicated structure. As a result, GSNMF has better performance than SNMF in identifying the memberships of samples. The final purpose of this paper is to perform safety monitoring using GSNMF through identifying the membership of the current sample.

Given a sample set $\mathbf{X}_l \in \mathbb{R}^{m\times n_l}$ where the membership of each sample in $\mathbf{X}_l$ is already known in advance, and a sample set $\mathbf{X}_u \in \mathbb{R}^{m\times n_u}$ where the membership of each sample in $\mathbf{X}_u$ is unknown. Without loss of generality, we suppose that each column of $\mathbf{X}_l$ and $\mathbf{X}_u$ is a sample. GSNMF attempts to construct a matrix factorization model as follow

$$[\mathbf{X}_l\ \mathbf{X}_u] = \mathbf{U}[\mathbf{V}_l\ \mathbf{V}_u] + \mathbf{E} \tag{3}$$

where matrix $\mathbf{U} \in \mathbb{R}^{m\times k}$ is known as a centroid matrix, $\mathbf{V}_u \in \mathbb{R}_+^{k\times n_u}$ is referred to as a membership indicator matrix with respect to $\mathbf{X}_u$, $\mathbf{E} \in \mathbb{R}^{m\times(n_l+n_u)}$ is an error matrix. The matrix $\mathbf{V}_l$ should be already known because the elements in $\mathbf{V}_l$ indicate the memberships of the samples in $\mathbf{X}_l$. As a result, the matrix $\mathbf{V}_l$ can be initialized in an understandable way, i.e., if i-th sample in $\mathbf{V}_l$ is from j-th cluster then $(\mathbf{V}_l)_{ji} = 1$, otherwise, $(\mathbf{V}_l)_{ji} = 0$. Actually, above initialization of $\mathbf{V}_l$ follows the clustering principle used by k-means algorithm.

Naturally, the unknown matrices $\mathbf{U}$ and $\mathbf{V}_u$ can be determined by solving the following constrained optimization problem.

$$\min_{\mathbf{U},\mathbf{V}_u\geq\mathbf{0}} J(\mathbf{U}, \mathbf{V}_u) = \|[\mathbf{X}_l\ \mathbf{X}_u] - \mathbf{U}[\mathbf{V}_l\ \mathbf{V}_u]\|_F^2 \tag{4}$$

To further improve the clustering performance of the model (3), we introduce a graph-based regularizer into model (3). Because we hope that the indicator matrix $\mathbf{V}$ can indicate the memberships of the samples in $\mathbf{X}$. Therefore, if two samples $\mathbf{x}_i$ and $\mathbf{x}_j$ in $\mathbf{X}$ are similar, then we hope that their membership indicators $\mathbf{v}_i$ and $\mathbf{v}_j$ are similar as well.

To this end, we construct a graph-based regularizer as follows

$$\begin{aligned} R &= \frac{1}{2}\sum_{i=1}^{N}\mathbf{W}_{ij}\left\|\mathbf{v}_i-\mathbf{v}_j\right\|_F^2 \\ &= \sum_{i=1}^{N}\mathbf{D}_{ii}\mathbf{v}_i^T\mathbf{v}_i-\sum_{ij=1}^{N}\mathbf{W}_{ij}\mathbf{v}_i^T\mathbf{v}_j \\ &= trace\left(\mathbf{V}\mathbf{D}\mathbf{V}^T\right)-trace\left(\mathbf{V}\mathbf{W}\mathbf{V}^T\right) \\ &= trace\left(\mathbf{V}\mathbf{L}\mathbf{V}^T\right) \\ &= trace\left([\mathbf{V}_l\ \mathbf{V}_u]\mathbf{L}[\mathbf{V}_l\ \mathbf{V}_u]^T\right) \\ &= trace\left(\begin{bmatrix}\mathbf{L}_1 & \mathbf{L}_2\\ \mathbf{L}_3 & \mathbf{L}_4\end{bmatrix}\begin{bmatrix}\mathbf{V}_l^T\mathbf{V}_l & \mathbf{V}_l^T\mathbf{V}_u\\ \mathbf{V}_u^T\mathbf{V}_l & \mathbf{V}_u^T\mathbf{V}_u\end{bmatrix}\right) \\ &= trace\left(\mathbf{L}_1\mathbf{V}_l^T\mathbf{V}_l+\mathbf{L}_2\mathbf{V}_u^T\mathbf{V}_l+\mathbf{L}_3\mathbf{V}_l^T\mathbf{V}_u+\mathbf{L}_4\mathbf{V}_u^T\mathbf{V}_u\right) \end{aligned} \tag{5}$$

where $\mathbf{L}_1, \mathbf{L}_2, \mathbf{L}_3$ and $\mathbf{L}_4$ are submatrices of $\mathbf{L}$ with appropriate dimensions, $\mathbf{D}_{ii} = \sum_j \mathbf{W}_{ij}$, $\mathbf{L} = \mathbf{D} - \mathbf{W}$ is called graph Laplacian, and

$$\mathbf{W}_{ij} = e^{-\frac{\left\|\mathbf{x}_i-\mathbf{x}_j\right\|_F^2}{\delta}} \tag{6}$$

Graph theory already told us that one can guarantee that if two samples $\mathbf{x}_i$ and $\mathbf{x}_j$ in $\mathbf{X}$ are closed then their memberships indicators $\mathbf{v}_i$ and $\mathbf{v}_j$ are also closed by minimizing R.

As a result, GSNMF problem reduces to solve the following optimization problem

$$\begin{aligned} &min\ J(\mathbf{U},\mathbf{V}_u) \\ &= \|[\mathbf{X}_l\ \mathbf{X}_u]-\mathbf{U}[\mathbf{V}_l\ \mathbf{V}_u]\|_F^2 - trace\left(\mathbf{\Phi}^T\mathbf{V}_u\right) \\ &\quad +\lambda trace\left(\mathbf{L}_1\mathbf{V}_l^T\mathbf{V}_l+\mathbf{L}_2\mathbf{V}_u^T\mathbf{V}_l+\mathbf{L}_3\mathbf{V}_l^T\mathbf{V}_u+\mathbf{L}_4\mathbf{V}_u^T\mathbf{V}_u\right) \\ &= \|\mathbf{X}_l-\mathbf{U}\mathbf{V}_l\|_F^2+\|\mathbf{X}_u-\mathbf{U}\mathbf{V}_u\|_F^2 - trace\left(\mathbf{\Phi}^T\mathbf{V}_u\right) \\ &\quad +\lambda trace\left(\mathbf{L}_1\mathbf{V}_l^T\mathbf{V}_l+\mathbf{L}_2\mathbf{V}_u^T\mathbf{V}_l+\mathbf{L}_3\mathbf{V}_l^T\mathbf{V}_u+\mathbf{L}_4\mathbf{V}_u^T\mathbf{V}_u\right) \end{aligned} \tag{7}$$

where $\mathbf{\Phi}$ is a Lagrange multiplier matrix associated with constraint $\mathbf{V}_u \geq \mathbf{0}$, and λ is a tradeoff parameter.

The partial derivative of $J(\mathbf{U},\mathbf{V}_u)$ with respect to $\mathbf{U}$ is

$$\frac{\partial J(\mathbf{U},\mathbf{V}_u)}{\partial \mathbf{U}} = 2\mathbf{U}[\mathbf{V}_l\ \mathbf{V}_u][\mathbf{V}_l\ \mathbf{V}_u]^T - 2\mathbf{X}[\mathbf{V}_l\ \mathbf{V}_u]^T.$$

Consider the following condition

$$\frac{\partial J(\mathbf{U},\mathbf{V}_u)}{\partial \mathbf{U}} = \mathbf{0}, \tag{8}$$

we have an update rule for $\mathbf{U}$ as follows

$$\begin{aligned} \mathbf{U} &= \mathbf{X}[\mathbf{V}_l\ \mathbf{V}_u]^T\left([\mathbf{V}_l\ \mathbf{V}_u][\mathbf{V}_l\ \mathbf{V}_u]^T\right)^{-1} \\ &= \mathbf{X}[\mathbf{V}_l\ \mathbf{V}_u]^T\left(\mathbf{V}_l\ \mathbf{V}_l^T+\mathbf{V}_u\mathbf{V}_u^T\right)^{-1} \end{aligned} \tag{9}$$

The partial derivative of $J(\mathbf{U},\mathbf{V}_u)$ with respect to $(\mathbf{V}_u)_{ij}$ is

$$\begin{aligned} &\frac{\partial J(\mathbf{U},\mathbf{V}_u)}{\partial\ (\mathbf{V}_u)_{ij}} \\ &= 2\left(\mathbf{U}^T\mathbf{U}\mathbf{V}_u\right)_{ij}-2\left(\mathbf{U}^T\mathbf{X}_u\right)_{ij}+\lambda\left(\mathbf{V}_l\mathbf{L}_2\right)_{ij} \\ &\quad +\lambda\left(\mathbf{V}_l\mathbf{L}_3^T\right)_{ij}+2\lambda\left(\mathbf{V}_u\mathbf{L}_4\right)_{ij}-\mathbf{\Phi}_{ij} \\ &= 2\left(\mathbf{U}^T\mathbf{U}\mathbf{V}_u\right)_{ij}-2\left(\mathbf{U}^T\mathbf{X}_u\right)_{ij}+2\lambda\left(\mathbf{V}_l\mathbf{L}_2\right)_{ij} \\ &\quad +2\lambda\left(\mathbf{V}_u\mathbf{L}_4\right)_{ij}-\mathbf{\Phi}_{ij} \end{aligned} \tag{10}$$

According to the following factorizations

$$\mathbf{U}^T\mathbf{U} = \left(\mathbf{U}^T\mathbf{U}\right)^+ - \left(\mathbf{U}^T\mathbf{U}\right)^- \tag{11}$$

and

$$\mathbf{U}^T\mathbf{X}_u = \left(\mathbf{U}^T\mathbf{X}_u\right)^+ - \left(\mathbf{U}^T\mathbf{X}_u\right)^- \tag{12}$$

where, for any matrix $\mathbf{A}$, $\mathbf{A}^+ = \frac{1}{2}(|\mathbf{A}|+\mathbf{A})$, $\mathbf{A}^- = \frac{1}{2}(|\mathbf{A}|-\mathbf{A})$, we have

$$\begin{aligned} &\frac{\partial J(\mathbf{U},\mathbf{V}_u)}{\partial\ (\mathbf{V}_u)_{ij}} \\ &= 2\left(\mathbf{U}^T\mathbf{U}\mathbf{V}_u\right)_{ij}-2\left(\mathbf{U}^T\mathbf{X}_u\right)_{ij}+2\lambda\left(\mathbf{V}_l\mathbf{L}_2\right)_{ij}+2\lambda\left(\mathbf{V}_u\mathbf{L}_4\right)_{ij} \\ &= 2\left(\left(\mathbf{U}^T\mathbf{U}\right)^+\mathbf{V}_u-\left(\mathbf{U}^T\mathbf{U}\right)^-\mathbf{V}_u\right)_{ij} \\ &\quad -2\left(\left(\mathbf{U}^T\mathbf{X}_u\right)^+-\left(\mathbf{U}^T\mathbf{X}_u\right)^-\right)_{ij} \\ &\quad +2\lambda\left(\mathbf{V}_l\mathbf{L}_2\right)_{ij}+2\lambda\left(\mathbf{V}_u\mathbf{L}_4\right)_{ij}-\mathbf{\Phi}_{ij} \end{aligned} \tag{13}$$

Since $\mathbf{V}_u$ is a nonnegative matrix, thus we have the KKT condition $\mathbf{\Phi}_{ij}(\mathbf{V}_u)_{ij}^2 = 0$. We have zero-gradient condition

$$\frac{\partial J(\mathbf{U},\mathbf{V}_u)}{\partial\ (\mathbf{V}_u)_{ij}} = 0. \tag{14}$$

According to the above conditions, we have an update rule for $(\mathbf{V}_u)_{ij}$ as follows

$$\begin{aligned} &(\mathbf{V}_u)_{ij} \\ &= (\mathbf{V}_u)_{ij} \\ &\quad \times\sqrt{\frac{\left((\mathbf{U}^T\mathbf{U})^-\mathbf{V}_u\right)_{ij}+\left(\mathbf{U}^T\mathbf{X}_u\right)_{ij}^+}{\left((\mathbf{U}^T\mathbf{U})^+\mathbf{V}_u\right)_{ij}+\left(\mathbf{U}^T\mathbf{X}_u\right)_{ij}^-+\lambda\left(\mathbf{V}_l\mathbf{L}_2\right)_{ij}+\lambda\left(\mathbf{V}_u\mathbf{L}_4\right)_{ij}}} \end{aligned} \tag{15}$$

Next, we will introduce an important conclusion that, for fixed $\mathbf{U}$, the objective function $J(\mathbf{U},\mathbf{V}_u)$ is non-increasing under update rule (15). Because the update rule (9) is an optimal solution to the optimization problem $min\ J(\mathbf{U},\mathbf{V}_u)$ for fixed $\mathbf{V}_u$. Thus, the objective $J(\mathbf{U},\mathbf{V}_u)$ is non-increasing if we apply the update rules (9) and (15) in turns, i.e., the GSNMF algorithm is convergent.

We will adopt auxiliary function method to prove the convergence of the GSNMF algorithm. The detailed definition of

an auxiliary function can be found in the literature [24]. The auxiliary function method is always used to prove the convergence of an algorithm. Because, if an auxiliary function of an objective function is non-increasing under an update rule then the objective function is also non-increasing under this update rule, i.e., the update rule is convergent.

The objective function $J(\mathbf{U}, \mathbf{V}_u)$ can be rewritten as

$$\begin{aligned} &J(\mathbf{U}, \mathbf{V}_u) \\ &= \|\mathbf{X}_l - \mathbf{U}\mathbf{V}_l\|_F^2 + trace\left(\mathbf{X}_u^T\mathbf{X}_u - 2\mathbf{X}_u^T\mathbf{U}\mathbf{V}_u + \mathbf{V}_u^T\mathbf{U}^T\mathbf{U}\mathbf{V}_u\right) \\ &\quad + \lambda trace\left(\mathbf{L}_1\mathbf{V}_l^T\mathbf{V}_l + \mathbf{L}_2\mathbf{V}_u^T\mathbf{V}_l + \mathbf{L}_3\mathbf{V}_l^T\mathbf{V}_u + \mathbf{L}_4\mathbf{V}_u^T\mathbf{V}_u\right) \end{aligned} \tag{16}$$

For any nonnegative matrix $\mathbf{V}'_u$, the following inequalities

$$\begin{aligned} &trace\left(\mathbf{V}_u^T(\mathbf{U}^T\mathbf{U})^+\mathbf{V}_u\right) \\ &\le \sum_{ij} \frac{\left((\mathbf{U}^T\mathbf{U})^+\mathbf{V}'_u\right)_{ij}(\mathbf{V}_u)_{ij}^2}{(\mathbf{V}'_u)_{ij}} \end{aligned} \tag{17}$$

$$\begin{aligned} &trace\left(\mathbf{V}_u^T(\mathbf{U}^T\mathbf{U})^-\mathbf{V}_u\right) \\ &= \sum_{ijk} (\mathbf{V}_u)_{ij}(\mathbf{U}^T\mathbf{U})_{ik}^-(\mathbf{V}_u)_{kj} \\ &\ge \sum_{ijk} (\mathbf{U}^T\mathbf{U})_{ik}^-(\mathbf{V}'_u)_{ij}(\mathbf{V}'_u)_{kj}\left(1 + \log\frac{(\mathbf{V}_u)_{ij}(\mathbf{V}_u)_{kj}}{(\mathbf{V}'_u)_{ij}(\mathbf{V}'_u)_{kj}}\right) \end{aligned} \tag{18}$$

$$\begin{aligned} &trace\left(\left(\mathbf{X}_u^T\mathbf{U}\right)^+\mathbf{V}_u\right) \\ &= \sum_{ij}\left(\mathbf{U}^T\mathbf{X}_u\right)_{ij}^+(\mathbf{V}_u)_{ij} \\ &\ge \sum_{ij}\left(\mathbf{U}^T\mathbf{X}_u\right)_{ij}^+(\mathbf{V}'_u)_{ij}\left(1 + \log\frac{(\mathbf{V}_u)_{ij}}{(\mathbf{V}'_u)_{ij}}\right) \end{aligned} \tag{19}$$

$$\begin{aligned} &trace\left(\left(\mathbf{X}_u^T\mathbf{U}\right)^-\mathbf{V}_u\right) \\ &= \sum_{ij}\left(\mathbf{U}^T\mathbf{X}_u\right)_{ij}^-(\mathbf{V}_u)_{ij} \\ &\le \sum_{ij}\left(\mathbf{U}^T\mathbf{X}_u\right)_{ij}^-\frac{(\mathbf{V}_u)_{ij}^2 + \left(\mathbf{V}'_u\right)_{ij}^2}{2(\mathbf{V}'_u)_{ij}} \end{aligned} \tag{20}$$

$$\begin{aligned} &trace\left(\mathbf{L}_2\mathbf{V}_u^T\mathbf{V}_l\right) \\ &= \sum_{ij}(\mathbf{V}_u)_{ij}(\mathbf{V}_l\mathbf{L}_2)_{ij} \\ &\le (\mathbf{V}_l\mathbf{L}_2)_{ij}\frac{(\mathbf{V}_u)_{ij}^2 + \left(\mathbf{V}'_u\right)_{ij}^2}{2(\mathbf{V}'_u)_{ij}} \end{aligned} \tag{21}$$

$$\begin{aligned} &trace\left(\mathbf{L}_3\mathbf{V}_l^T\mathbf{V}_u\right) \\ &= \sum_{ij}(\mathbf{V}_u)_{ij}\left(\mathbf{V}_l\mathbf{L}_3^T\right)_{ij} \\ &\le \left(\mathbf{V}_l\mathbf{L}_3^T\right)_{ij}\frac{(\mathbf{V}_u)_{ij}^2 + \left(\mathbf{V}'_u\right)_{ij}^2}{2(\mathbf{V}'_u)_{ij}} \end{aligned} \tag{22}$$

and

$$trace\left(\mathbf{L}_4\mathbf{V}_u^T\mathbf{V}_u\right) \le \left(\mathbf{V}'_u\mathbf{L}_4\right)_{ij}\frac{(\mathbf{V}_u)_{ij}^2}{(\mathbf{V}'_u)_{ij}} \tag{23}$$

demonstrate that

$$\begin{aligned} &F(\mathbf{V}_u, \mathbf{V}'_u) \\ &= \|\mathbf{X}_l - \mathbf{U}\mathbf{V}_l\|_F^2 + \lambda trace\left(\mathbf{L}_1\mathbf{V}_l^T\mathbf{V}_l\right) \\ &\quad + \lambda\left(\mathbf{V}_l\mathbf{L}_2\right)_{ij}\frac{(\mathbf{V}_u)_{ij}^2 + \left(\mathbf{V}'_u\right)_{ij}^2}{2(\mathbf{V}'_u)_{ij}} \\ &\quad + \lambda\left(\mathbf{V}_l\mathbf{L}_3^T\right)_{ij}\frac{(\mathbf{V}_u)_{ij}^2 + \left(\mathbf{V}'_u\right)_{ij}^2}{2(\mathbf{V}'_u)_{ij}} \\ &\quad + \lambda\left(\mathbf{V}'_u\mathbf{L}_4\right)_{ij}\frac{(\mathbf{V}_u)_{ij}^2}{(\mathbf{V}'_u)_{ij}} + \sum_{ij}\frac{\left((\mathbf{U}^T\mathbf{U})^+\mathbf{V}'_u\right)_{ij}(\mathbf{V}_u)_{ij}^2}{(\mathbf{V}'_u)_{ij}} \\ &\quad - \sum_{ijk}(\mathbf{U}^T\mathbf{U})_{ik}^-\left(\mathbf{V}'_u\right)_{ij}\left(\mathbf{V}'_u\right)_{kj}\left(1 + \log\frac{(\mathbf{V}_u)_{ij}(\mathbf{V}_u)_{kj}}{(\mathbf{V}'_u)_{ij}(\mathbf{V}'_u)_{kj}}\right) \\ &\quad + 2\sum_{ij}\left(\mathbf{U}^T\mathbf{X}_u\right)_{ij}^-\frac{(\mathbf{V}_u)_{ij}^2 + \left(\mathbf{V}'_u\right)_{ij}^2}{2(\mathbf{V}'_u)_{ij}} \\ &\quad - 2\sum_{ij}\left(\mathbf{U}^T\mathbf{X}_u\right)_{ij}^+\left(\mathbf{V}'_u\right)_{ij}\left(1 + \log\frac{(\mathbf{V}_u)_{ij}}{(\mathbf{V}'_u)_{ij}}\right) \end{aligned} \tag{24}$$

is an auxiliary function of objective function $J(\mathbf{U}, \mathbf{V}_u)$.

Because inequalities (17)-(23) hold, thus $F(\mathbf{V}_u, \mathbf{V}'_u) \ge J(\mathbf{U}, \mathbf{V}_u)$ and $F(\mathbf{V}_u, \mathbf{V}_u) = J(\mathbf{U}, \mathbf{V}_u)$ also hold. As a result, it is an obvious fact that $F(\mathbf{V}_u, \mathbf{V}'_u)$ is an auxiliary function of $J(U, \mathbf{V}_u)$. The relation between an objective function and its auxiliary function is demonstrated by Figure 1 [24].

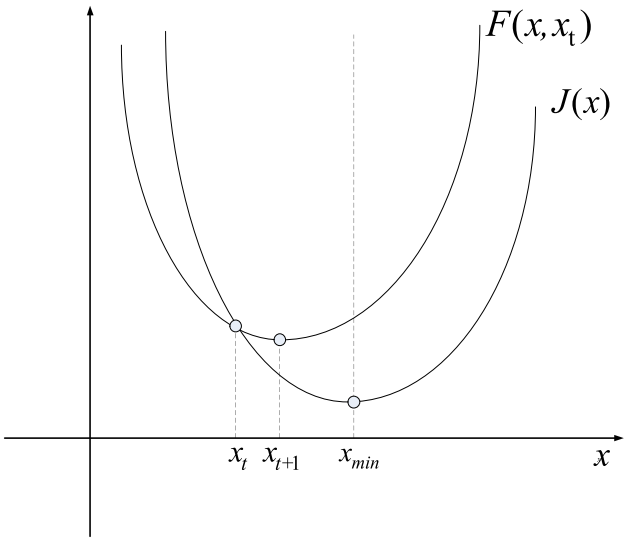

FIGURE 1. The relation between an objective function J(x) and its auxiliary function F(x,xt).

TABLE 1. Algorithm of the GSNMF.

Inputs: Sample matrix $\mathbf{X}=[\mathbf{X}_l\ \mathbf{X}_u]$ where $\mathbf{X}_l$ and $\mathbf{X}_u$ consist of labeled and unlabeled samples, respectively; the cluster number k of the samples in $[\mathbf{X}_l\ \mathbf{X}_u]$; the parameter δ in the function (6); the tradeoff parameter λ in the objective function (7).
Outputs: Matrices $\mathbf{U}$ and $\mathbf{V}_u$.
Steps: 1 Calculate graph Laplacian matrix $\mathbf{L}=\mathbf{D}-\mathbf{W}$ 2 Initialize $\mathbf{V}_l$ if i-th sample in $\mathbf{V}_l$ is from j-th cluster, then $(\mathbf{V}_l)_{ji}=1$, otherwise, $(\mathbf{V}_l)_{ji}=0$, and initialize $\mathbf{V}_u$ with a nonnegative matrix randomly. 3 loop: 4 Update $\mathbf{U}$ using update rule (9) 5 Update $\mathbf{V}_u$ using update rule (15) 6 end loop until convergence

The partial derivative of $F(\mathbf{V}_u, \mathbf{V}'_u)$ with respect to $(\mathbf{V}_u)_{ij}$ is

$$\begin{aligned}&\frac{\partial F(\mathbf{V}_u,\mathbf{V}'_u)}{\partial\,(\mathbf{V}_u)_{ij}}\\&=\lambda\,(\mathbf{V}_l\mathbf{L}_2)_{ij}\frac{(\mathbf{V}_u)_{ij}}{(\mathbf{V}'_u)_{ij}}+\lambda\left(\mathbf{V}_l\mathbf{L}_3^T\right)_{ij}\frac{(\mathbf{V}_u)_{ij}}{(\mathbf{V}'_u)_{ij}}\\&\quad+2\lambda\left(\mathbf{V}'_u\mathbf{L}_4\right)_{ij}\frac{(\mathbf{V}_u)_{ij}}{(\mathbf{V}'_u)_{ij}}\\&\quad+2\frac{\left(\mathbf{U}^T\mathbf{X}_u\right)^-_{ij}(\mathbf{V}_u)_{ij}}{(\mathbf{V}'_u)_{ij}}-2\frac{\left(\mathbf{U}^T\mathbf{X}_u\right)^+_{ij}(\mathbf{V}'_u)_{ij}}{(\mathbf{V}_u)_{ij}}\\&\quad+2\frac{\left(\left(\mathbf{U}^T\mathbf{U}\right)^+\mathbf{V}'_u\right)_{ij}(\mathbf{V}_u)_{ij}}{(\mathbf{V}'_u)_{ij}}-2\frac{\left(\left(\mathbf{U}^T\mathbf{U}\right)^-\mathbf{V}'_u\right)_{ij}(\mathbf{V}'_u)_{ij}}{(\mathbf{V}_u)_{ij}}\end{aligned}\tag{25}$$

Let

$$\frac{\partial F(\mathbf{V}_u,\mathbf{V}'_u)}{\partial\,(\mathbf{V}_u)_{ij}}=0,\tag{26}$$

one can obtain an update rule identical to (15), which immediately completes the proof of the convergence of GSNMF algorithm.

The GSNMF algorithm is described in Table 1 for readers to better understand it.

III. SAFETY MONITORING BY IDENTIFYING THE MEMBERSHIP OF THE CURRENT SAMPLE

For any newly coming sample $\mathbf{x}_{new}$, it should follow a relation with its membership indicator $\mathbf{v}_{new}$ as follows

$$\mathbf{x}_{new}\approx\mathbf{U}\mathbf{v}_{new}\tag{27}$$

Moreover, the new graph-based regularizer becomes

$$\begin{aligned}&trace\left([\mathbf{V}\ \mathbf{v}_{new}]\mathbf{L}_{new}[\mathbf{V}\ \mathbf{v}_{new}]^T\right)\\&=trace\left(\begin{bmatrix}(\mathbf{L}_{new})_1&(\mathbf{L}_{new})_2\\(\mathbf{L}_{new})_3&(\mathbf{L}_{new})_4\end{bmatrix}\begin{bmatrix}\mathbf{V}^T\mathbf{V}&\mathbf{V}^T\mathbf{v}_{new}\\\mathbf{v}_{new}^T\mathbf{V}&\mathbf{v}_{new}^T\mathbf{v}_{new}\end{bmatrix}\right)\\&=trace\Big((\mathbf{L}_{new})_1\,\mathbf{V}^T\mathbf{V}+(\mathbf{L}_{new})_2\,\mathbf{v}_{new}^T\mathbf{V}\\&\quad+(\mathbf{L}_{new})_3\,\mathbf{V}^T\mathbf{v}_{new}+(\mathbf{L}_{new})_4\,\mathbf{v}_{new}^T\mathbf{v}_{new}\Big)\end{aligned}\tag{28}$$

Similarly, the indicator $\mathbf{v}_{new}$ can be determined by solving the following constrained optimization problem

$$\begin{aligned}min\ J(\mathbf{v}_{new})=&\|\mathbf{x}_{new}-\mathbf{U}\mathbf{v}_{new}\|_F^2-\boldsymbol{\varphi}^T\mathbf{v}_{new}\\&+\lambda trace\Big((\mathbf{L}_{new})_1\,\mathbf{V}^T\mathbf{V}+(\mathbf{L}_{new})_2\,\mathbf{v}_{new}^T\mathbf{V}\\&+(\mathbf{L}_{new})_3\,\mathbf{V}^T\mathbf{v}_{new}+(\mathbf{L}_{new})_4\,\mathbf{v}_{new}^T\mathbf{v}_{new}\Big)\end{aligned}\tag{29}$$

where $\boldsymbol{\varphi}$ is a Lagrange multiplier vector associated with constraint $\mathbf{v}_{new}\geq\mathbf{0}$.

The partial derivative of $J(\mathbf{v}_{new})$ with respect to $(\mathbf{v}_{new})_j$ is

$$\begin{aligned}\frac{\partial J(\mathbf{v}_{new})}{\partial\,(\mathbf{v}_{new})_j}=&\,2\lambda\,(\mathbf{V}\,(\mathbf{L}_{new})_2)_j+2\lambda\,(\mathbf{v}_{new}\,(\mathbf{L}_{new})_4)_j-\boldsymbol{\varphi}_j\\&+2\left(\left(\mathbf{U}^T\mathbf{U}\right)^+\mathbf{v}_{new}-\left(\mathbf{U}^T\mathbf{U}\right)^-\mathbf{v}_{new}\right)_j\\&-2\left(\left(\mathbf{U}^T\mathbf{x}_{new}\right)^+-\left(\mathbf{U}^T\mathbf{x}_{new}\right)^-\right)_j\end{aligned}\tag{30}$$

According to

$$\frac{\partial J(\mathbf{v}_{new})}{\partial\,(\mathbf{v}_{new})_j}=0,$$

one can obtain an update rule for $\mathbf{v}_{new}$ as follows in (31), shown at the bottom of the page.

Finally, the membership of the sample $\mathbf{x}_{new}$ can be identified by its indicator $\mathbf{v}_{new}$. If the training samples contains both normal sample and all types of abnormal samples then one can know what the membership of $\mathbf{x}_{new}$ is.

$$(\mathbf{v}_{new})_j=(\mathbf{v}_{new})_j\times\sqrt{\frac{\left((\mathbf{U}^T\mathbf{U})^-\mathbf{v}_{new}\right)_j+\left(\mathbf{U}^T\mathbf{v}_{new}\right)^+_j}{\left((\mathbf{U}^T\mathbf{U})^+\mathbf{v}_{new}\right)_j+\left(\mathbf{U}^T\mathbf{v}_{new}\right)^-_j+\lambda\,(\mathbf{V}\,(\mathbf{L}_{new})_2)_j+\lambda\,(\mathbf{v}_{new}\,(\mathbf{L}_{new})_4)_j}}\tag{31}$$

IV. CASE STUDY

Steel enterprises need to mark important parameters, the mintmark, size, batch number, date, and other information on the surface of their products, to meet the standard management rules. Traditionally, the marking work is done by workers. Because of the bad working conditions such as high temperature, hazardous and noxious substances, and repetitive work for a long time in fast speed, it is unavoidable for workers to mark occasionally the wrong label on the products. So, the robotic-arm based marking system is designed for replacing human labor to enhance marking efficiency with high quality.

Robotic-arm has the advantages of fast movement speed, large impact force, flexible track and large working range. However, mechanical failure and control failure may occur to the robotic-arm. So, the working area of the robotic-arm is a very dangerous place for workers. Therefore, the purpose of the safety monitoring system is to protect workers from injury. Moreover, we hope that the safety monitoring system will alert the workers who enter the work zone of robotic-arm. To implement safety monitoring, we collect some images including normal and abnormal images. With the aid of these images, the safety monitoring task reduce to determine the memberships of a newly coming image. To be specific, if the image has a same membership as the normal images, then no safety risks are detected. On the contrary, if the image has a same membership as the abnormal images, then safety risks are detected.

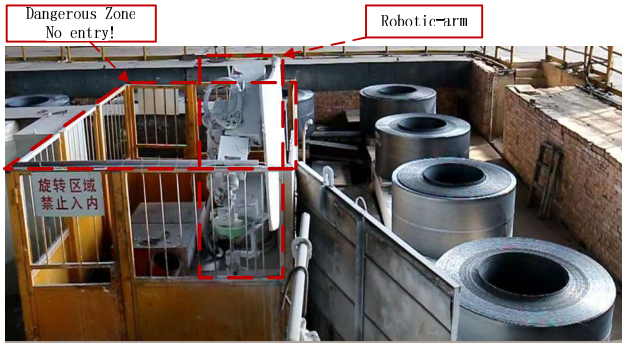

FIGURE 2. Normal sample of marking process with robotic-arm and its' dangerous zone.

Figure 2 is a sample of normal images, while Figure 3 consists of two samples of abnormal images since a worker appeared in the dangerous zone. i.e., the robotic-arm's working region. Obviously, the region we are interested in the images is the robotic-arm's working zone, and all others regions are regarded as background with less safety information. As a result, in the preprocessing phase, we extract only the robotic-arm's working zone in the images and transform the extracted color images into gray images and norm the size to 550×500.

Figure 4 contains two sample images from both the preprocessed normal and abnormal images, respectively.

To demonstrate the capabilities of the proposed methods, NMF, SNMF, convex nonnegative matrix factorization

FIGURE 3. Two samples of abnormal images.

(a)normal sample image (b)abnormal sample image

FIGURE 4. Samples of preprocessed image of monitoring zone.

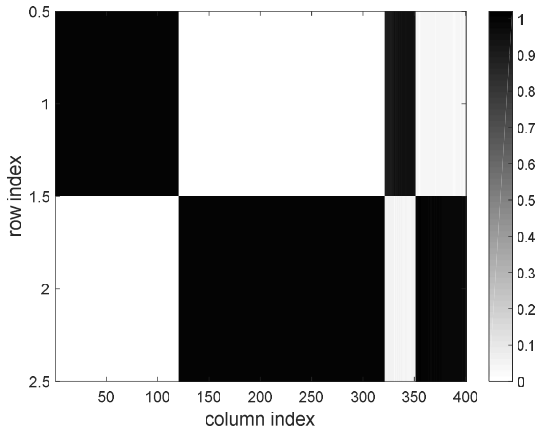

FIGURE 5. Monitoring result by GSNMF.

(CNMF) [23], graph-regularized nonnegative matrix factorization (GNMF) [21], and transfer semi-nonnegative matrix factorization (TSNMF) [19] are also considered for comparison in the experiment. As a result, six algorithms namely NMF, SNMF, CNMF, GNMF, TSNMF, and GSNMF were

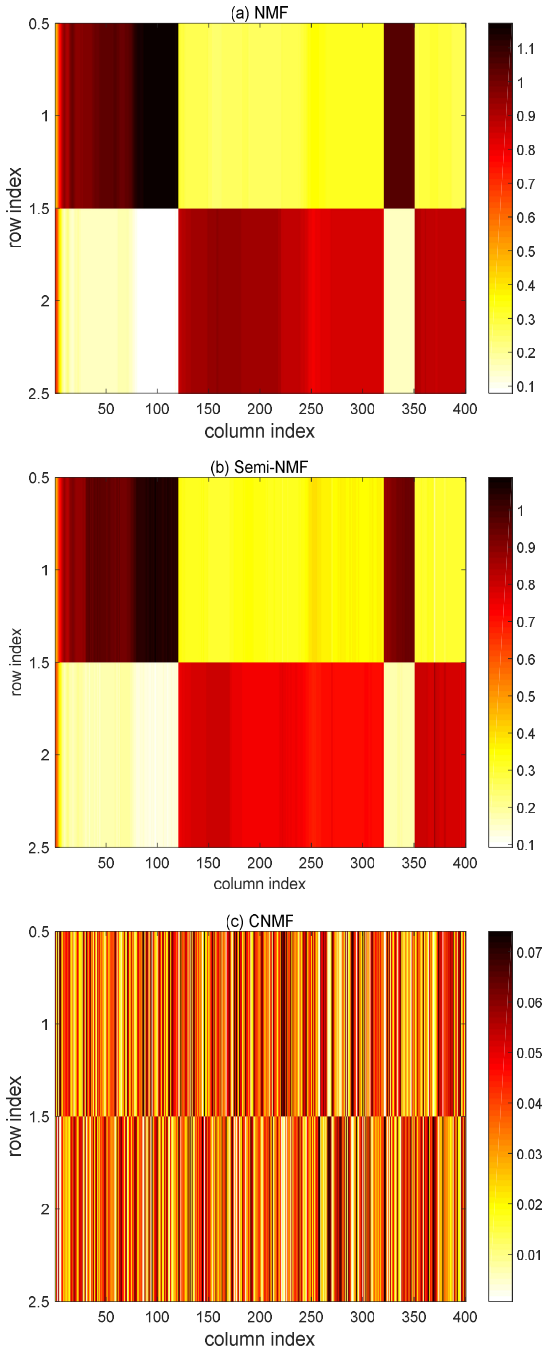

FIGURE 6. Monitoring results by NMF, Semi-NMF and CNMF.

used to develop safety monitoring approaches to identify the memberships of the test images. In this experiment, a total of 400 preprocessed images were collected, including 150 normal images and 250 abnormal images. We use five-fold cross validation method to evaluate the performance of the proposed method. The data set is divided into five subsets, and the holdout method is repeated for five times. In each time, one of the five subsets is used as the test set and the other four subsets are put together to form a training set. Then the average indexes across all five trials is computed as shown in Table 2. The indexes are accuracy, precision, recall, F1-score, and run time.

TABLE 2. Comparisons of performance indexes of different algorithms.

Algorithm\Index	Accuracy (%)	Precision (%)	Recall (%)	F1-Score	Run Time (s)
NMF	99	100	98	99	254
SNMF	81	81	81	81	37
CNMF	51	37	42	39	3
GNMF	99	100	98	99	437
TSNMF	99	100	98	99	266
GSNMF	99	100	97	99	218

The monitoring result by GSNMF is demonstrated in Figure 5. According to the indicator matrix, as shown in Figure 5, we can conclude that the proposed approach can successfully and accurately identify the memberships of the 30 normal images and 50 abnormal images.

The monitoring results using NMF and SNMF are given by Figure 6-(a) and 6-(b), respectively. During the experiment, we found that the accuracy of monitoring results are highly dependent on initialization of matrices $\mathbf{U}$ and $\mathbf{V}$ for NMF and SNMF-based monitoring methods. Although NMF performs well as TSNMF and GSNMF, it sometimes give the results in inverse form. Because the NMF is not a supervised learning method, we do not take the result in inverse form as a wrong result. So, we just selected a result in normal form among these case studies, as shown in Figure 6-(a). Although SNMF-based monitoring approach can identify the memberships of the 30 normal images and 50 abnormal images sometimes, the monitoring results are not sharp enough.

Figure 6-(c) indicates that the CNMF-based monitoring approach totally failed to identify the memberships of the 30 normal images and 50 abnormal images. The reason why the CNMF failed in this experiment may be that the centroids generated by the CNMF are far away from each group of samples since the values in the indicator matrix are relatively small.

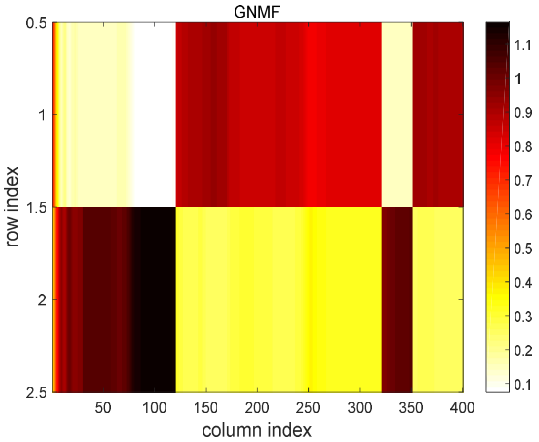

FIGURE 7. Monitoring results by GNMF.

Besides NMF, CNMF and SNMF, we also take GNMF and TSNMF proposed by [21] and [19], respectively

for comparison. Figure 7 and 8 show the experiment results by GNMF and TSNMF, respectively. Note that GNMF give an inverse experiment result compared with the other methods. TSNMF shows a correct experiment result, which is considerable close to the experiment result from GSNMF. Compared to TSNMF, GSNMF consumes less time.

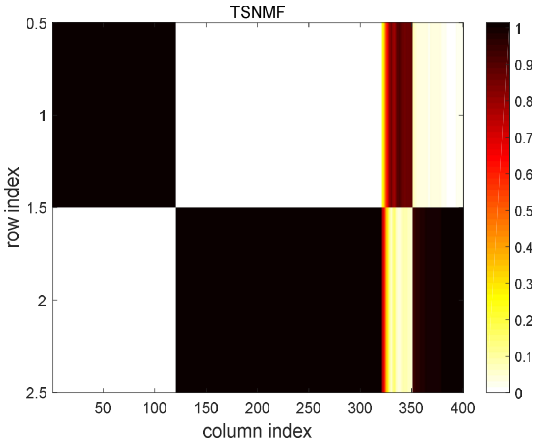

FIGURE 8. **Monitoring results by TSNMF.**

In conclusion, the experimental results indicate that the proposed GSNMF-based safety monitoring approach can accurately identify the membership of the testing images, which means that any potential risks for safety in the steel coil marking process can be found by the proposed monitoring approach. Moreover, the proposed approach outperforms the other monitoring approaches such as SNMF- and CNMF-based monitoring approaches. Although NMF, TSNMF, and GSNMF-based monitoring approaches generate higher monitoring precision than the other monitoring approaches, GSNMF has a higher computational efficiency compared with NMF and TSNMF.

V. CONCLUSIONS

We have proposed GSNMF to perform safety monitoring and have successfully applied it to a steel coil marking process. Compared with the existing approaches, the new approaches have some unique features. For example, the proposed approach can fully make use of the labelled data to implement semi-supervised learning in the framework of NMF, and the geometry of sample data is maintained at the same time. In addition, the nonlinear structure of sample data can be described, and make the low dimension representation of samples have a better separability. We have also introduced the safety monitoring methods developed by GSNMF, which make use of images, instead of traditional data collected from different types of sensors, to find the safety risk for workers. The use of images allows us to perform monitoring more easier than traditional methods since images are easy to collect. Finally, the superiorities of our approach over the existing approaches have been demonstrated through a case study on a steel coil marking process.

REFERENCES

[1] S. X. Ding, "Data-driven design of monitoring and diagnosis systems for dynamic processes: A review of subspace technique based schemes and some recent results," *J. Process Control*, vol. 24, no. 2, pp. 431–449, Feb. 2014.
[2] S. Fan, Y. W. Zhang, Y. Z. Zhang, and Z. Fang, "Motion process monitoring using optical flow–based principal component analysis-independent component analysis method," *Adv. Mech. Eng.*, vol. 9, no. 11, pp. 1–12, Nov. 2017.
[3] S. J. Qin, "Statistical process monitoring: Basics and beyond," *J. Chemometrics*, vol. 17, nos. 8–9, pp. 480–502, 2003.
[4] S. Yin, S. X. Ding, X. C. Xie, and H. Luo, "A review on basic data-driven approaches for industrial process monitoring," *IEEE Trans. Ind. Electron.*, vol. 61, no. 11, pp. 6418–6428, Jan. 2014.
[5] J. Dong, M. Wang, X. Zhang, L. Ma, and K. Peng, "Joint data-driven fault diagnosis integrating causality graph with statistical process monitoring for complex industrial processes," *IEEE Access*, vol. 5, pp. 25217–25225, Oct. 2017.
[6] Q. Yan, J. Huang, C. Xiong, Z. Yang, and Z. Yang, "Data-driven human-robot coordination based walking state monitoring with cane-type robot," *IEEE Access*, vol. 6, pp. 8896–8908, Feb. 2018.
[7] G. Li, C. F. Alcala, S. J. Qin, and D. Zhou, "Generalized reconstruction-based contributions for output-relevant fault diagnosis with application to the Tennessee Eastman process," *IEEE Trans. Control Syst. Technol.*, vol. 19, no. 5, pp. 1114–1127, Sep. 2011.
[8] G. Li, S. J. Qin, and D. Zhou, "Geometric properties of partial least squares for process monitoring," *Automatica*, vol. 46, no. 1, pp. 204–210, Jan. 2010.
[9] G. Li, S. J. Qin, and D. Zhou, "A new method of dynamic latent-variable modeling for process monitoring," *IEEE Trans. Ind. Electron.*, vol. 61, no. 11, pp. 6438–6445, Nov. 2014.
[10] Q. Wen, Z. Ge, and Z. Song, "Data-based linear Gaussian state-space model for dynamic process monitoring," *AIChE J.*, vol. 58, no. 12, pp. 3763–3776, Dec. 2012.
[11] D. Zhou, G. Li, and S. J. Qin, "Total projection to latent structures for process monitoring," *AIChE J.*, vol. 56, no. 1, pp. 168–178, 2010.
[12] Z. Ge, Z. Song, and F. Gao, "Review of recent research on data-based process monitoring," *Ind. Eng. Chem. Res.*, vol. 52, no. 10, pp. 3543–3562, Mar. 2013.
[13] T. Wu, F. Li, C. Yang, and W. Gui, "Event-based fault detection filtering for complex networked jump systems," *IEEE/ASME Trans. Mechatronics*, vol. 23, no. 2, pp. 497–505, Apr. 2018.
[14] D. D. Lee and H. S. Seung, "Learning the parts of objects by non-negative matrix factorization," *Nature*, vol. 401, no. 6755, pp. 788–791, Oct. 1999.
[15] Y.-X. Wang and Y.-J. Zhang, "Nonnegative matrix factorization: A comprehensive review," *IEEE Trans. Knowl. Data Eng.*, vol. 25, no. 6, pp. 1336–1353, Jun. 2013.
[16] N. Li and Y. Yang, "Statistical process monitoring based on modified nonnegative matrix factorization," *J. Intell. Fuzzy Syst.*, vol. 28, no. 3, pp. 1359–1370, 2015.
[17] X. Li, Y. Yang, and W. Zhang, "Statistical process monitoring via generalized non-negative matrix projection," *Chemometric Intell. Lab. Syst.*, vol. 121, pp. 15–25, Feb. 2013.
[18] X.-B. Li, Y.-P. Yang, and W.-D. Zhang, "Fault detection method for non-Gaussian processes based on non-negative matrix factorization," *Asia-Pacific J. Chem. Eng.*, vol. 8, no. 3, pp. 362–370, May 2013.
[19] Q. Jia, Y. Zhang, and W. Chen, "Simultaneous fault detection and isolation based on transfer semi-nonnegative matrix factorization," *Ind. Eng. Chem. Res.*, vol. 58, no. 19, pp. 8184–8194, May 2019.
[20] L. Zhang, Z. Liu, L. Wang, and J. Pu, "Adaptive graph regularization discriminant nonnegative matrix factorization for data representation," *IEEE Access*, vol. 7, pp. 112756–112766, 2019.
[21] D. Cai, X. He, J. Han, and T. S. Huang, "Graph regularized nonnegative matrix factorization for data representation," *IEEE Trans. Pattern Anal. Mach. Intell.*, vol. 33, no. 8, pp. 1548–1560, Aug. 2011.
[22] H. Liu, Z. Wu, D. Cai, and T. S. Huang, "Constrained nonnegative matrix factorization for image representation," *IEEE Trans. Pattern Anal. Mach. Intell.*, vol. 34, no. 7, pp. 1299–1311, Jul. 2012.
[23] C. H. Q. Ding, T. Li, and M. I. Jordan, "Convex and semi-nonnegative matrix factorizations," *IEEE Trans. Pattern Anal. Mach. Intell.*, vol. 32, no. 1, pp. 45–55, Jan. 2010.
[24] D. D. Lee and H. S. Seung, "Algorithms for non-negative matrix factorization," in *Proc. Adv. Neural Inf. Process. Syst.*, vol. 13, 2011, pp. 556–562.

SONG FAN received the B.S. degree in electrical and control engineering from Liaoning Technical University, Fuxin, China, in 2006, and the master's degree in control theory and control engineering from Northeastern University, Shenyang, China, in 2008, where he is currently pursuing the Ph.D. degree in control theory and control engineering. Besides, he is also working as the Deputy Director of the School of Electronic and Information Engineering, University of Science and Technology Liaoning. His current research interests include data-driven fault detection and diagnosis, machine learning, and machine vision.

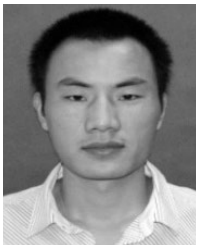

QILONG JIA received the B.S. degree in electrical engineering and automation from Liaoning University, Shenyang, China, in 2010, and the master's degree in control theory and control engineering from Dalian Maritime University, Dalian, China, in 2013. He is currently pursuing the Ph.D. degree in control theory and control engineering with Northeastern University, Shenyang. His current research interests include process modeling with multivariate statistical techniques, and data-driven fault detection and diagnosis.

WAN SHENG CHENG received the Ph.D. degree from the School of Mechatronics Engineering, Harbin Institute of Technology, Harbin, China, in 2008. He is currently working as the Director of the Intelligent Manufacturing Engineering Technology Center, University of Science and Technology Liaoning. His current research interests include signal processing, intelligent equipment, and robot application. He is a member of the Robotics Committee of the Chinese Association of Automation.